DOI: 10.1111/jdv.15329 JEADV

ORIGINAL ARTICLE

Morphological classification of melanoma metastasis with reflectance confocal microscopy

F. Farnetani,[1] M. Manfredini,[1,2,*] S. Longhitano,[1] J. Chester,[1] K. Shaniko,[1] E. Cinotti,[3] L. Mazzoni,[4] M. Venturini,[5] A. Manganoni,[5] C. Longo,[1,6] L. Reggiani-Bonetti,[7] L. Giannetti,[8] P. Rubegni,[3] P. Calzavara-Pinton,[5] I. Stanganelli,[4,9] J.L. Perrot,[10] G. Pellacani[1]

[1]Division of Dermatology, Department of Surgical, Medical, Dental and Morphological Sciences with Interest transplant, Oncological and Regenerative Medicine, University of Modena and Reggio Emilia, Modena, Italy
[2]Division of Dermatology, University of Ferrara, Ferrara, Italy
[3]Department of Medical, Surgical, and Neurological Science, Dermatology Section, University of Siena, S Maria alle Scotte Hospital, Siena, Italy
[4]Skin Cancer Unit, IstitutoTumori Romagna (IRST), Meldola, Italy
[5]Division of Dermatology, SpedaliCivili University Hospital, Brescia, Italy
[6]Skin Cancer Unit, Arcispedale Santa Maria Nuova-IRCCS, Reggio Emilia, Italy
[7]Department of Pathology, University of Modena and Reggio Emilia, Modena, Italy
[8]Department of Surgical, Medical, Dental and Morphological Sciences with Interest Transplant, Oncological and Regenerative Medicine, University of Modena and Reggio Emilia, Modena, Italy
[9]Division of Dermatology, Department of Clinical and Experimental Medicine, University of Parma, Parma, Italy
[10]Department of Dermatology, University Hospital of Saint-Etienne, Saint-Etienne, France
*Correspondence: M. Manfredini. E-mail: manfredini07@gmail.com

Abstract

Background Cutaneous malignant melanoma metastases differential diagnosis is challenging, as clinical and dermoscopic features can simulate primary melanoma or other benign or malignant skin neoplasms, and *in-vivo* reflectance confocal microscopy could assist. Our aim was to identify specific reflectance confocal microscopy features for cutaneous malignant melanoma metastases, and epidermal and dermal involvement.

Methods A retrospective, multicentre observational study of lesions with proven cutaneous malignant melanoma metastases diagnosis between January 2005 and December 2016. Lesions were retrospectively assessed according to morphological features observed at reflectance confocal microscopy. Potential homogeneous subgroups of epidermal or dermal involvement were investigated with cluster analysis.

Results Cutaneous malignant melanoma metastases (51 lesions in 29 patients) exhibited different frequencies of features according to metastasis dermoscopy patterns. Lesions classified at dermoscopy with nevus-like globular and non-globular patterns were more likely to be epidermotropic, showing characteristics of epidermal and dermal involvement at reflectance confocal microscopy. Other dermoscopy pattern classifications were more likely to be dermotropic, showing characteristics od dermal involvement at reflectance confocal microscopy. Distinguishing features at reflectance confocal microscopy included irregular (78%) and altered (63%) epidermis, pagetoid infiltration (51%), disarranged junctional architecture (63%), non-edged papillae (76%), dense and sparse, and cerebriform nests in the upper dermis (74%), and vascularity (51%). Cluster analysis identified three groups, which were retrospectively correlated with histopathological diagnoses of dermotropic and epidermotropic diagnoses ($P < 0.001$). The third cluster represents lesions with deep dermis morphological changes, which were too deep for evaluation with reflectance confocal microscopy.

Conclusions Specific reflectance confocal microscopy features of cutaneous malignant melanoma metastases for correct diagnosis, and subtype diagnosis, seem achievable in most cases where morphological alterations are located above the deep dermis.

Received: 20 August 2018; Accepted: 12 October 2018

Conflict of interest

Prof. Pellacani Giovanni received honoraria for seminars on confocal microscopy from MAVIG GmbH (Germany).

Funding source

The study was supported by a grant of NET (Italian Ministry of Health, NET 2011-02347213).

Introduction

Melanoma can metastasize to any organ, and metastatic malignant melanoma is most commonly observed on the skin in the dermis and subcutaneous tissue, and less frequently in visceral organs.[1] The reported incidence of cutaneous malignant melanoma metastases (CMMMs) ranges from 2 to 20%[2] and represents the first clinical manifestation of the disease in approximately 2–8% of patients with melanoma.[2] CMMM differential diagnosis is challenging, as clinical and dermoscopic features can simulate primary melanoma or other benign or malignant skin neoplasms,[3–10] but correct diagnosis is essential to clinical staging, therapeutic management and prognosis. Histological features of CMMMs have been documented, underlining the difficulties in selected cases of differential diagnosis from a primary lesion.[11–17]

In a clinical setting, the initial evaluation of cutaneous lesions is performed with dermoscopy, which can evidence unusual patterns associated with either malignant neoplasms or benign lesions.[4,18] However, differential diagnosis is confirmed with the gold standard histopathology. Most CMMMs involve the dermis and subcutaneous tissue (dermotropic), but in some cases lesions can be more superficial (epidermotropic). The histomorphological spectrum of CMMMs has been widely documented.[14]

Technological innovation has provided clinicians with the opportunity to obtain an *in-vivo* study of skin tissue up to 200 μm, by means of a non-invasive, optical biopsy at almost histologic resolution with the reflectance confocal microscopy (RCM). Common features of nevi and malignant melanoma (MM) identified at RCM have already been correlated with histopathologic criteria[19–26] and its usage has proven to enhance diagnostic accuracy compared to dermoscopy alone for melanocytic lesions.[27–30] However, specific diagnostic RCM CMMM criteria have not yet been outlined in literature. The current study aims to identify and describe specific CMMM morphological features as evidenced at RCM, for the differential diagnoses of CMMMs, and to identify epidermal and dermal involvement.

Materials and methods

A retrospective, multicentre, observational study design was used to select and assess all lesions with proven CMMM diagnosis at histopathology, registered with RCM and included in a dedicated database at the 4 referral institutes, between January 2005 and December 2016. Further inclusion criteria specified the requirement for a complete set of high quality dermoscopic and RCM images. Participating sites included the University Hospital of Modena (Italy), University Hospital of Brescia (Italy), Scientific Romagnolo Institute for Tumor (IRST IRCCS, Italy), and the University Hospital of Saint Etienne (France). All images were collected and forwarded to a single centre for retrospective analysis, performed at the same time by three dermatologists (F.F, S.L, M.M). In the case of a failed consensus, a further fourth investigator was engaged (G.P.).

The study was approved by the Institutional Reviewed Board of Modena and the investigation was conduced in accordance with the Declaration of Helsinki.

Dermoscopic analysis

All dermoscopic images of the lesions, obtained with the DermLite FOTO System (DermLite Photo 3Gen_ LLC, San Juan Capistrano, CA, USA), were retrospectively classified, according to melanoma metastases dermoscopic patterns established by Costa *et al.*[18]: blue-nevus like, globular nevus-like, non-globular nevus-like, angioma-like, vascular or unspecific patterns.

Reflectance confocal microscopy analysis

Reflectance confocal microscopy images were obtained with a Vivascope 1500 or 3000 (Caliber, New York, USA, distributed in Europe by MAVIG GmbH, Munich, Germany) using an 830-nm laser at a maximum power of 20 mW, depending upon centre preference. Method and acquisition settings have been previously described.[20] A complete set of at least three Vivablock® mosaics (epidermal layer, dermo-epidermal junction and the upper dermis with Vivascope 1500) or five Vivastack® images with the Vivascope 3000, were evaluated. RCM criteria for melanocytic lesions and the relevant definitions for the classification of the lesions are outlined in Table S1.[19–25]

Histology

The histopathologic examination of the metastases was performed on haematoxylin-eosin staining slides ruled out from the archives of the Pathologic Anatomy – University of Modena and Reggio Emilia. Morphologically, circumscribed non-encapsulated nodular metastases located in the dermis and with no epidermis involvement were defined as dermotropic CMMMs; differently, those characterized by a spread of pagetoid cells throughout the overlying epidermis and upper dermis were classified as epidermotropic CMMMs. In selected cases, the epidermal pagetoid spread was confirmed by immunohistochemical stains (S100 – polyclonal antibody; Dako; 1/3000 dilution, and HMB-45 – monoclonal antibody; Dako; 1/50 dilution).

Statistical analysis

Descriptive statistics and complete case analysis were used for all comparisons between groups. Pearson's chi-squared test and Fisher's exact test were used for associations between variables and groups. A hierarchical cluster analysis was performed to identify potential homogeneous subgroups of CMMMs within the cohort. All variables, excluding histological diagnoses, were included to clustering and lesions without a full set of data were excluded ($n = 1$). To minimize the total within-cluster variance, Ward's main clustering methods were used. The optimal number of clusters was determined according to Calinski and

Harabasz stopping method[31] (k); the pseudo-F index indicates the appropriate number of clusters, where larger values of pseudo-F indicate more distinct clustering, and considerations of interpretation of the data in the clinical context by expert dermatologists.[32] After selecting the optimal number of clusters, the parameters were analysed and compared using the χ^2 test. Subsequently, the patient's codes were broken and data were compared to histopathological diagnoses. All statistical analyses were performed using the STATA® software, version 14 (StataCorp. 2015. Stata Statistical Software: Release 14. College Station, TX, USA: StataCorp LP.). $P < 0.05$ was considered statistically significant.

Results

A total of 51 CMMMs from 29 patients were included in the study. CMMMs were grouped according to dermoscopy metastasis patterns and frequencies of RCM parameters. Data are displayed in Table 1.

At RCM, the most frequent pattern observed in the epidermis in most groups was the irregular broadened pattern. Most of the CMMMs classified with the nevus-like globular and non-globular patterns at dermoscopy exhibited pleomorphic pagetoid infiltration, but interestingly this pattern was less represented in most lesions classified at dermoscopy as blue nevus-like, angioma-like and vascular patterns ($P = 0.023$).

At the dermal-epidermal junction (DEJ), papillae were remarkably different between the angioma-like pattern and the other dermoscopy patterns. Non-edged papillae were identified in all nevus-like globular (6/6, 100%)) and non-globular patterns (8/8, 100%), and most vascular (12/15, 80%) and unspecific patterns (8/10, 80%) whereas edged papillae were evidenced in 75% of lesions classified with the angioma-like pattern (3/4; $P = 0.011$).

The presence of junctional nests was mostly observed in the nevus-like globular (5/6, 83%) and non-globular patterns (7/8, 87%) but were absent in over two-thirds of angioma-like (3/4, 75%) and vascular patterns (10/15, 67%). In the upper dermis, cerebriform nests and the presence of vascularity were prevalent in most lesion characterized with angioma-like (2/4, 50% and 4/4, 100%, respectively) and vascular patterns (10/15, 67% and 13/15, 87%, respectively), There was a complete and almost complete absence of cerebriform nests associated with nevus-like non-globular pattern (0/8, 0%) and nevus-like globular pattern (1/6, 17%) respectively. Dense and sparse dermal nests were mainly associated with the nevus-like globular (4/6, 67%) and non-globular patterns (5/8, 62%).

Features identified as statistically significantly different between the groups included the epidermis patterns ($P = 0.002$), pagetoid infiltration ($P = 0.023$), junctional architecture ($P = 0.017$), non-edged papillae ($P = 0.011$), junctional nests ($P = 0.046$), nests in the upper dermis ($P = 0.043$) and vascularity ($P = 0.002$), Table 1.

Hierarchical cluster analysis

All CMMMs with a complete set of parameters were classified according to dermoscopy classifications and RCM parameters (one lesion was excluded). To determine the number of clusters, the largest pseudo-F statistic (Table S2) considering the clinical meaningfulness of the cluster produced, created a three-cluster solution selection. The presence of lesions with the absence of all RCM parameters, due to the limited laser depth penetration of RCM, was grouped together in the three-cluster solution, producing a more meaningful analysis of the data. The three clusters provided by the hierarchical cluster analysis determined 150 L^2 values, Figure S1. Descriptive statistics of dermoscopic and RCM parameters in each cluster are presented in Table 2.

Cluster 1 included 18 lesions, which had mostly been classified at histology as epidermotropic (12 cases, 66.7%). These 12 lesions represented 100% of all epidermotropic lesions diagnosed at histology. Most lesions had been classified at dermoscopy as nevus like globular (6/18, 33%), non-globular (7/18, 39%) and blue nevus-like (5/18, 28%) CMMMs. RCM analysis of the epidermis, evidenced a mostly irregular broadened honeycomb pattern (13/18, 72%), with epidermal disruption (14/18, 78%) and pagetoid infiltration (12/18, 67%). At the DEJ, the disarranged architecture was most obvious (13/18, 72%) with non-edged papillae (17/18, 94%), associated with a strong presence of junctional nests (15/18, 83%) and all atypical cell types (15/18, 83%). At the dermis, dense and sparse dermal nests (11/18, 61%) with bright and plump inflammatory infiltrates covering more than half of the lesions' surface (13/18, 72%), and an absence of both prominent vascularity and collagen (12/18, 67% respectively) were witnessed, Fig. 1.

Cluster 2 involved 29 lesions, which were all diagnosed at histology as dermotropic (29/38, 76.3% of all dermotropic lesions diagnosed in this cohort). At dermoscopy, these lesions were mostly classified as vascular (15/29, 52%), unspecific (9/29, 31%), and some were angioma-like (4/29, 14%). At RCM, this cluster could be differentiated from Cluster 1 primarily by the presence of cerebriform nests in over half the lesions in the upper dermis and vascularity (15/29, 52% and 20/29, 69%, respectively). Further, there was the absence of junctional nests in the DEJ and pagetoid infiltration in the epidermis in over half of the lesions (20/29, 69% and 15/29, 52%, respectively), Fig. 2.

Cluster 3 included 3 lesions, all classified at histology as dermotropic CMMMs. At dermoscopy, these lesions were all classified as blue nevus-like. At RCM evaluation, none of these lesions exhibited any atypical features (0/3, 0%). Therefore, the epidermis illustrated regular cobblestone architecture with the absence of pagetoid infiltration. The DEJ showed a disarranged architecture with edged papillae and a marked absence of junctional nests. The dermis of all lesions was without any atypical cells or nests, inflammatory infiltrates, prominent vascularity or collagen, Fig. 3

Table 1 Frequencies of RCM parameters in CMMMs at dermoscopy

	Melanoma metastases dermoscopic patterns							
	Blue nevus-like pattern	Nevus-like globular pattern	Nevus-like non-globular pattern	Angioma-like pattern	Vascular pattern	Unspecific pattern	Total	
	8	6	8	4	15	10	51	
RCM parameters	*N* (%)	*N* (%)	*N* (%)	*N* (%)	*N* (%)	*N* (%)	*N* (%)	*P*-value
Epidermis								
Regular cobblestone	3 (37.5)	0 (0)	0 (0)	0 (0)	0 (0)	1 (10)	4 (7.8)	0.002
Regular honeycombed	0 (0)	0 (0)	1 (12.5)	3 (75)	2 (13.3)	1 (10)	7 (13.7)	
Irregular cobblestone	0 (0)	2 (33.3)	3 (37.5)	0 (0)	1 (6.7)	0 (0)	6 (11.8)	
Irregular broadened	5 (62.5)	4 (66.7)	4 (50)	1 (25)	12 (80)	8 (80)	34 (66.7)	
Epidermis alteration								
Absent	4 (50)	1 (16.7)	2 (25)	3 (75)	5 (33.3)	4 (40)	19 (37.3)	0.357
Disruption	3 (37.5)	5 (83.3)	6 (75)	1 (25)	7 (46.7)	6 (60)	28 (54.9)	
Ulceration	1 (12.5)	0 (0)	0 (0)	0 (0)	3 (20)	0 (0)	4 (7.8)	
Pagetoid infiltration								
Absent	6 (75)	1 (16.7)	3 (37.5)	4 (100)	9 (60)	2 (20)	25 (49)	0.023
Dendritic	0 (0)	1 (16.7)	0 (0)	0 (0)	3 (20)	0 (0)	4 (7.8)	
Roundish	1 (12.5)	1 (16.7)	0 (0)	0 (0)	2 (13.3)	4 (40)	8 (15.7)	
Pleomorphic	1 (12.5)	3 (50)	5 (62.5)	0 (0)	1 (6.7)	4 (40)	15 (29.4)	
Junctional architecture								
Ringed	4 (50)	0 (0)	0 (0)	2 (50)	3 (20)	2 (20)	11 (21.6)	0.017
Meshwork	0 (0)	0 (0)	2 (25)	0 (0)	0 (0)	1 (10)	3 (5.9)	
Clod	0 (0)	0 (0)	3 (37.5)	0 (0)	0 (0)	2 (20)	5 (9.8)	
Disarranged	4 (50)	6 (100)	3 (37.5)	2 (50)	12 (80)	5 (50)	32 (62.7)	
Papillae								
Edged	4 (50)	0 (0)	0 (0)	3 (75)	3 (20)	1 (10)	11 (21.6)	0.011
Non-edged	4 (50)	6 (100)	8 (100)	1 (25)	12 (80)	8 (80)	39 (76.5)	
Junctional nests								
Absent	5 (62.5)	1 (16.7)	1 (12.5)	3 (75)	10 (66.7)	6 (60)	26 (51)	0.046
Present	3 (37.5)	5 (83.3)	7 (87.5)	1 (25)	5 (33.3)	3 (30)	24 (47.1)	
Atypical cells								
Absent	3 (37.5)	1 (16.7)	2 (25)	1 (25)	0 (0)	3 (30)	10 (19.6)	0.333
Dendritic	0 (0)	1 (16.7)	0 (0)	0 (0)	0 (0)	0 (0)	1 (2)	
Roundish	1 (12.5)	1 (16.7)	2 (25)	1 (25)	8 (53.3)	2 (20)	15 (29.4)	
Pleomorphic	4 (50)	3 (50)	4 (50)	2 (50)	7 (46.7)	4 (40)	24 (47.1)	
Nest in upper dermis								
Absent	4 (50)	0 (0)	2 (25)	0 (0)	0 (0)	3 (30)	9 (17.6)	0.043
Dermal dense nests	0 (0)	1 (16.7)	1 (12.5)	0 (0)	0 (0)	1 (10)	3 (5.9)	
Dense and sparse dermal nests	2 (25)	4 (66.7)	5 (62.5)	2 (50)	5 (33.3)	2 (20)	20 (39.2)	
Cerebriform	2 (25)	1 (16.7)	0 (0)	2 (50)	10 (66.7)	3 (30)	18 (35.3)	
Inflammation								
Absent	3 (37.5)	1 (16.7)	5 (62.5)	2 (50)	2 (13.3)	2 (20)	16 (31.4)	0.291
Present	5 (62.5)	5 (83.3)	3 (37.5)	2 (50)	12 (80)	7 (70)	34 (66.7)	
Vascularity								
Absent	5 (62.5)	4 (66.7)	7 (87.5)	0 (0)	2 (13.3)	6 (60)	24 (47.1)	0.002
Present	3 (37.5)	2 (33.3)	1 (12.5)	4 (100)	13 (86.7)	3 (30)	26 (51)	
Collagen								
Absent	7 (87.5)	3 (50)	5 (62.5)	1 (25)	5 (33.3)	5 (50)	26 (51)	0.270
Reticulated collagen fibres	1 (12.5)	1 (16.7)	1 (12.5)	0 (0)	1 (6.7)	0 (0)	4 (7.8)	
Large bright bundles	0 (0)	2 (33.3)	2 (25)	3 (75)	9 (60)	4 (40)	20 (39.2)	

Table 2 Descriptive statistics of dermoscopic and RCM parameters in clusters analysis

	Cluster 1 18 *N* (%)	Cluster 2 29 *N* (%)	Cluster 3 3 *N* (%)	Total 50 *N* (%)	*P*-value χ^2
Histology*					
Epidermotropic CMMM	12 (67)	0 (0)	0 (0)	12 (24)	<0.001
Dermotropic CMMM	6 (33)	29 (100)	3 (100)	38 (76)	
Melanoma metastases dermoscopic patterns					
Blue nevus-like pattern	5 (28)	0 (0)	3 (100)	8 (16)	<0.001
Nevus-like globular pattern	6 (33)	0 (0)	0 (0)	6 (12)	
Nevus-like non-globular pattern	7 (39)	1(3)	0 (0)	8 (16)	
Angioma-like pattern	0 (0)	4 (14)	0 (0)	4 (8)	
Vascular pattern	0 (0)	15 (52)	0 (0)	15 (30)	
Unspecific pattern	0 (0)	9 (31)	0 (0)	9 (18)	
RCM parameters:					
Epidermis					
Regular cobblestone	0 (0)	1 (3)	3 (100)	4 (8)	<0.001
Regular honeycombed	0 (0)	7 (24)	0 (0)	7 (14)	
Irregular cobblestone	5 (28)	1 (3)	0 (0)	6 (12)	
Irregular broadened	13 (72)	20 (69)	0 (0)	33 (66)	
Epidermis alteration					
Absent	3 (17)	12 (41)	3 (100)	18 (36)	0.048
Disruption	14 (78)	14 (48)	0 (0)	28 (56)	
Ulceration	1 (6)	3 (10)	0 (0)	4 (8)	
Pagetoid infiltration					
Absent	6 (33)	15 (52)	3 (100)	24 (48)	0.150
Dendritic	1 (6)	3 (10)	0 (0)	4 (8)	
Roundish	2 (11)	6 (21)	0 (0)	8 (16)	
Pleomorphic	9 (50)	5 (17)	0 (0)	14 (28)	
Junctional architecture					
Ringed	1 (6)	6 (21)	0 (0)	7 (14)	0.019
Meshwork	2 (11)	1 (3)	0 (0)	3 (6)	
Clod	2 (11)	3 (10)	0 (0)	5 (10)	
Disarranged	13 (72)	19 (66)	3 (100)	35 (70)	
Papillae					
Edged	1 (6)	7 (24)	3 (100)	11 (22)	0.001
Non-edged	17 (94)	22 (76)	0 (0)	39 (78)	
Junctional nests					
Absent	3 (17)	20 (69)	3 (100)	26 (52)	0.001
Present	15 (83)	9 (31)	0 (0)	24 (48)	
Atypical cells					
Absent	3 (17)	4 (14)	3 (100)	10 (20)	0.008
Dendritic	1 (6)	0 (0)	0 (0)	1 (2)	
Roundish	3 (17)	12 (41)	0 (0)	15 (30)	
Pleomorphic	11 (61)	13 (45)	0 (0)	24 (48)	
Nest in upper dermis					
Absent	3 (17)	3 (10)	3 (100)	9 (18)	0.002
Dermal dense nests	1 (6)	2 (7)	0(0)	3 (6)	
Dense and sparse dermal nests	11 (61)	9 (31)	0 (0)	20 (40)	
Cerebriform	3 (17)	15 (52)	0 (0)	18 (36)	
Inflammation					
Absent	5 (28)	8 (28)	3 (100)	16 (32)	0.034
Present	13 (72)	21 (72)	0 (0)	34 (68)	

Table 2 *Continued*

	Cluster 1 18 *N* (%)	Cluster 2 29 *N* (%)	Cluster 3 3 *N* (%)	Total 50 *N* (%)	*P*-value χ^2
Vascularity					
Absent	12 (67)	9 (31)	3 (100)	24 (48)	0.011
Present	6 (33)	20 (69)	0 (0)	26 (52)	
Collagen					
Absent	12 (67)	11 (38)	3 (100)	26 (52)	0.017
Reticulated collagen fibres	3 (17)	1 (3)	0 (0)	4 (8)	
Large bright bundles	3 (17)	17 (59)	0 (0)	20 (40)	

*Parameter not considered in Cluster Analysis.

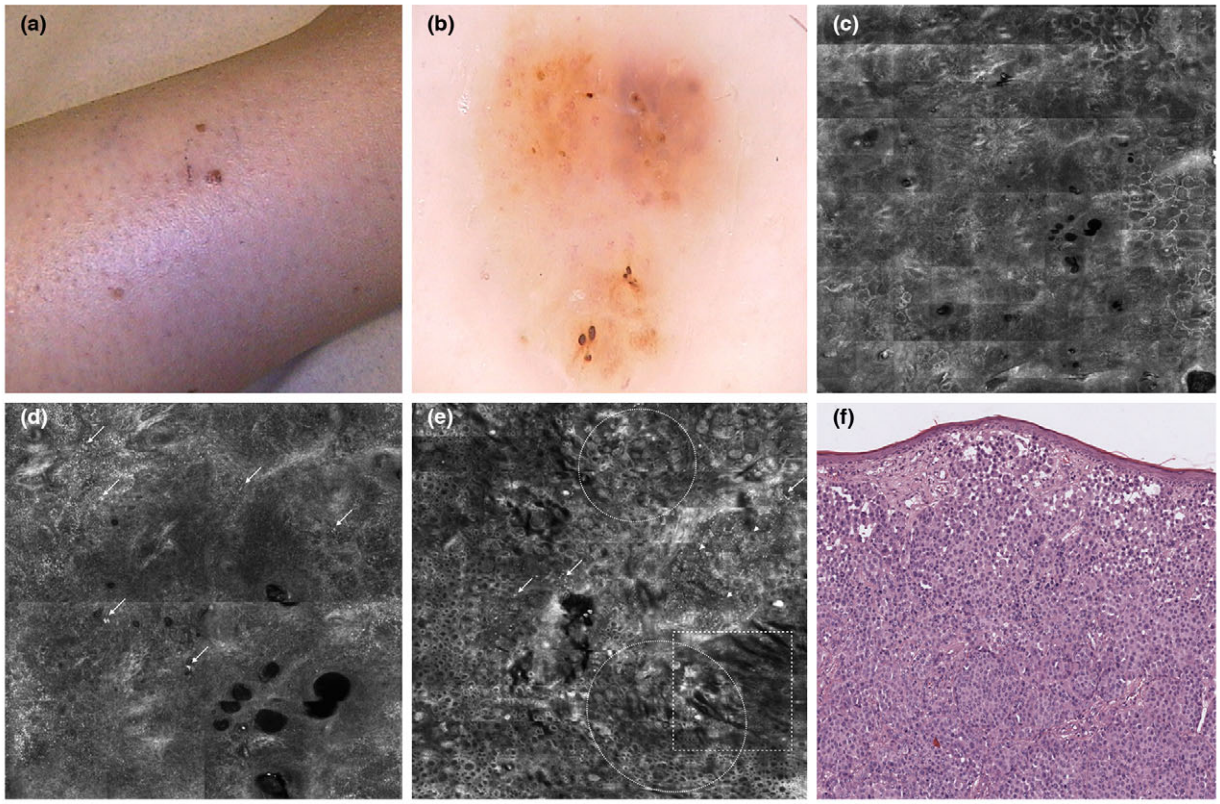

Figure 1 Clinical image of an epidermotropic CMMM located on the left leg of a female patient (a). The lesion, classified nevus-like globular type by dermoscopy, showed homogeneous pigmentation, a few dots and globules and fine irregular vessels (b). Overview of the RCM mosaic showing epidermal disruption and pagetoid infiltration (c). Magnified images of the previous RCM mosaic, illustrating pleomorphic pagetoid cells in the epidermis (white arrows) (d). Overview of the RCM mosaic at the DEJ, showing disarranged architecture with non-edged papillae (dashed white ellipses), associated with junctional nests (dashed white rectangle), atypical cells (white arrows), dense and sparse nests with bright inflammatory infiltrates (white arrow-heads) and the absence of both prominent vascularity and collagen (e). A dome-shaped nodule composed by various-sized nests of atypical epithelioid melanocytes exhibiting pagetoid spread in the epidermis (H&E, ×20) (f).

Chi-squared analysis was used to confirm the parameters that were able to discriminate between clusters resulting statistically significant for most for the parameters evaluated, as shown in Table 2. Of note, all parameters were statistically significant, but the various forms of pagetoid infiltration did not prove to be of assistance in determining cluster type.

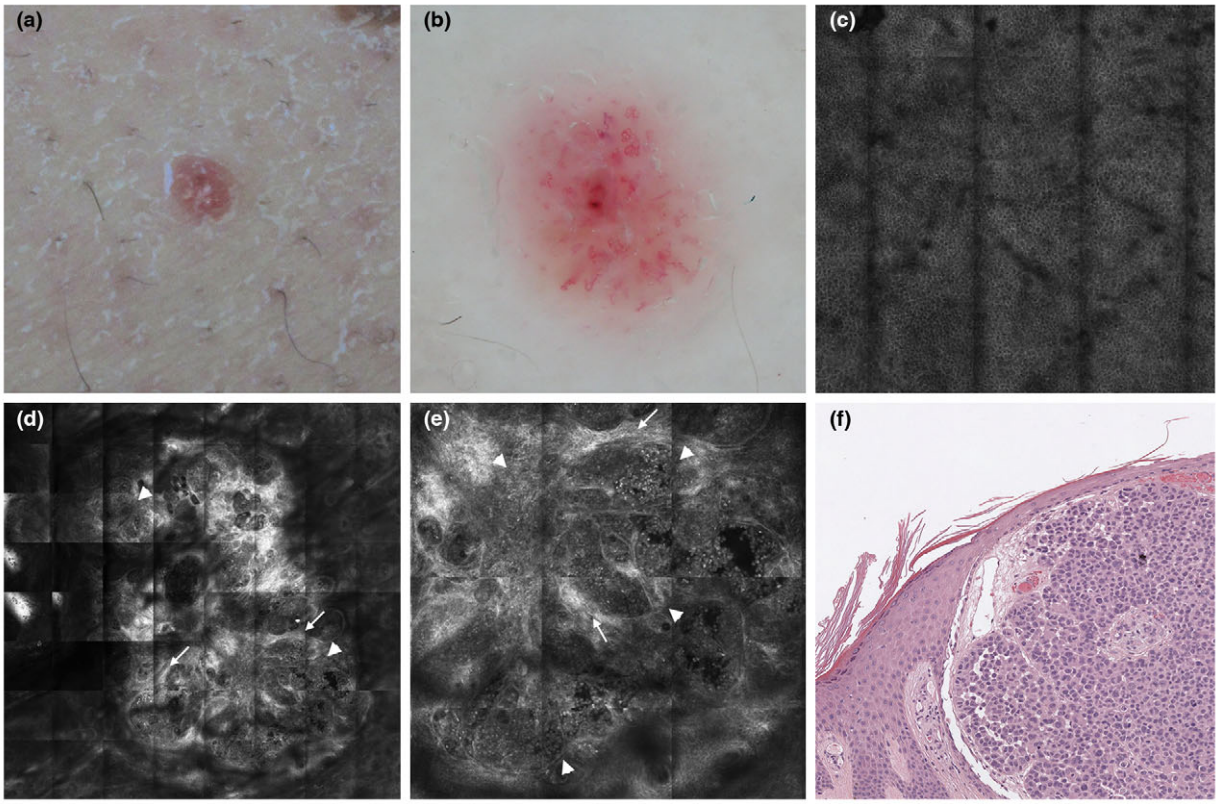

Figure 2 Clinical image of a dermotropic CMMM located on the left leg of a female patient (a). Dermoscopically characterized as a vascular type lesion, corkscrew atypical vessels and milky red areas (b). Overview of the RCM mosaic of the spinous layer, showing regular honeycomb pattern and a marked absence of pagetoid infiltration (c). Overview of the RCM mosaic of the upper dermis, showing disarranged architecture with non-edged papillae, associated with dense and sparse dermal nests, some of them with cerebriform shape (white arrow-heads) (d). Magnifications of the previous RCM mosaics, showing a cerebriform nest (white arrow-heads), many atypical cells and thick collagen bundles in the dermis (white arrows) (e). Well-circumscribed nodule in the dermis with no pagetoid spread in the epidermis (H&E, ×10) (f).

Discussion

Clinically CMMMs can be mistaken for benign or malignant neoplasms, due to the similarities in appearance observed at dermoscopy. The difficulty of differential diagnosis at dermoscopy, is underlined by the classification of metastatic lesions according to characteristics associated with other benign and malignant skin neoplasms, such as "nevus-like" and "angioma-like"[4,18] with the substantial risk of misdiagnosis in some lesions, with dramatic consequences.[4,18] Therefore, histology is the current gold standard for CMMM diagnoses, which, as Plaza *et al.*[14] suggest requires careful clinical history to establish correct diagnosis. RCM, which has been proven to be able to distinguish CMMMs with dermal involvement from other nodular lesions,[20] could be useful in *in-vivo* study of the dermis and subcutaneous tissue of suspect lesions. To date, the usefulness in identifying CMMMs at RCM according to defined parameters has not yet been outlined and there are only single case reports that described RCM features of melanoma metastases.[33]

In the current study, typical RCM melanocytic criteria were used to retrospectively assess histologically proven CMMMs. Analyses were organized according to the lesions' dermoscopic patterns. Atypical RCM patterns were evident in almost all CMMMs, in different frequencies according to dermoscopic pattern types. In general, the nevus-like globular and non-globular patterns had atypical RCM patterns in the epidermal and dermal layers, whereas the angioma-like, vascular and unspecific types had more marked atypia in the dermis. The group of blue-nevus like lesions exhibited some features of epidermal and dermal involvement

It has been proven that histology is able to distinguish the differential dermal and epidermal involvement in CMMMs.[14] The presence of circumscribed, non-encapsulated nodules in the dermis is considered indicative of dermotropic CMMMs, whereas epidermotropic lesions are characterized by a spread of tumour cells throughout the epidermis and dermis. Specifically, the dermotropic pattern shows a nodular neoplasm in the

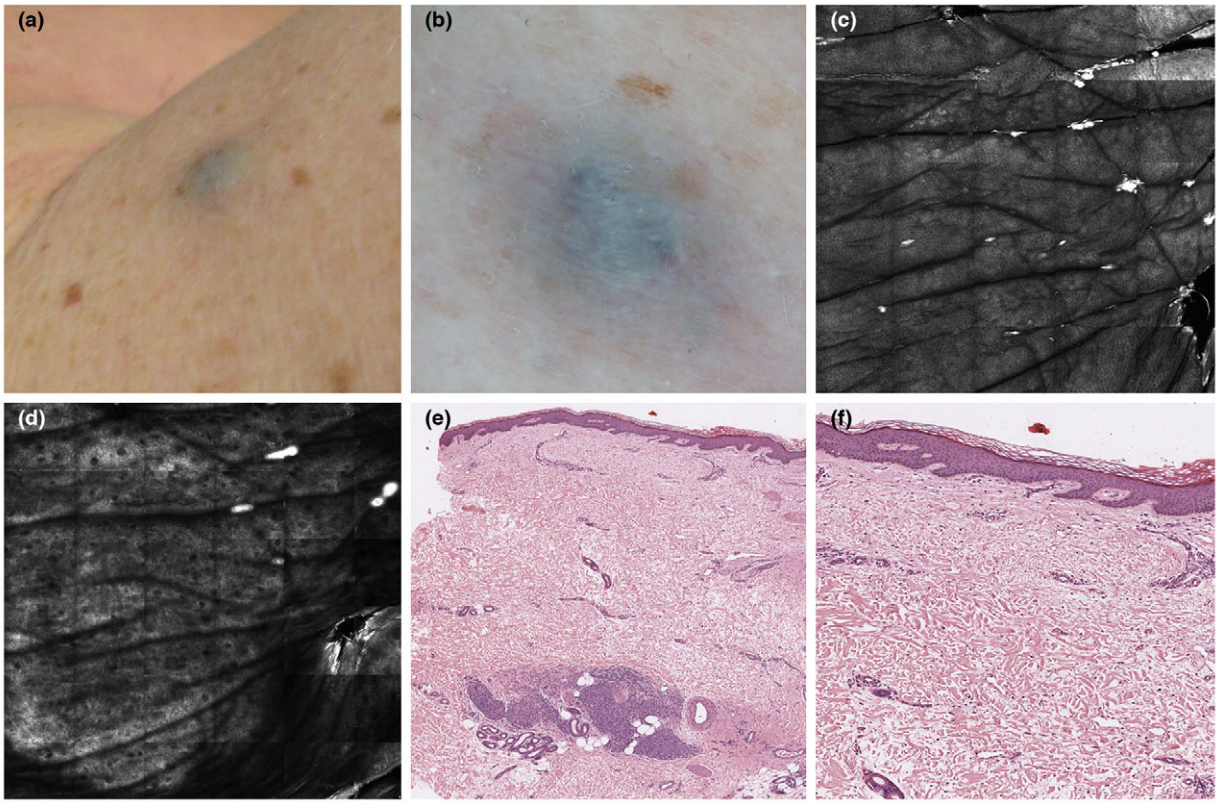

Figure 3 Clinical image of a deep dermotropic CMMM of the left shoulder of a female patient (a). Dermoscopically the lesion was classified as blue nevus-like, showing homogeneous blue pigmentation (b). Overview of the RCM mosaic of the spinous layer, showing regular honeycomb pattern and absence of pagetoid infiltration (c). Overview of the RCM mosaic of the upper dermis, showing non-edged papillae without any junctional or dermal nests (d). A small dermal nodule with clusters of atypical epithelioid melanocytes. The overlying epidermis was tumour-free (H&E, ×10) (e and f).

reticular or deep dermis, without a junctional component. The atypical melanocytes display striking pleomorphism, and occasionally there is the involvement of a well-formed epidermal collarete. Alternatively, epidermotropic CMMMs are identified by the marked epidermotropism, with an equal or greater involvement in the dermis.[11,12,14,16] To date, histopathologic CMMM subclassifications have not yet been correlated to RCM features.

Cluster analysis was performed to investigate any potential homogeneous groups. Three groups of CMMMs, according to the frequencies of RCM features were formed and following the breaking of patient codes, data were compared to histopathological diagnoses.

Cluster 1 included lesions dermoscopically classified as nevus-like globular and non-globular and the majority of the blue-nevus like lesions. The high presence of pagetoid cells and atypical dendric, roundish and pleomorphic cells with few cases of cerebriform nests ($n = 3$) characterized this group. CMMMs at histology with marked epidermotropic involvement, pagetoid spread in the epidermis (visualized at RCM as pagetoid cells) and the presence of "atypical melanocytes within the dermis having equal size or broader than intradermal component," (visualized at RCM as atypical cells) have been associated with epidermotropic CMMMs.[14] Therefore, the contemporary presence of pagetoid cells in the epidermis and atypical cells in the dermis[34] seem to correlate with the histological description of epidermotropic CMMMs by Plaza *et al.*[14] Almost two-thirds of the lesions included in this cluster were diagnosed at histopathology as epidermotropic CMMM and represented 100% of all epidermotropic histological proven CMMMs.

Cluster 2 included lesions more frequently classified at dermoscopy with angioma-like, vascular and unspecific patterns. The lesions were characterized by the highly evident presence of cerebriform nests in the dermis and the absence or rare presence of pagetoid cells in the epidermis, rare junctional nests and vascularization. It has already been demonstrated that the cerebriform nests visualized at RCM correlate to "dermal nest melanoma" and histology defined "non-encapsulated nodules,"[34,35,36] as indicative of dermotropic CMMMs.[14] All lesions

(100%) in Cluster 2 were confirmed dermotropic CMMMs at histology.

Cluster 3 only included three lesions, in which RCM analysis did not identify any signs of atypia in the epidermis, junction or dermis; all three lesions were confirmed at histology as dermotropic CMMMs.

Therefore, the only dermoscopic classification to be separated at Cluster analysis was the blue nevus-like. Five of the eight lesions were included in Cluster 1 despite 4 of the blue-nevus like being histopathologically classified as dermotropic CMMMs. These lesions evidenced both epidermal and dermal involvement; epidermal features included an irregular epidermis, disarranged DEJ architecture and inflammation. The remaining blue nevus-like lesions did not exhibit any features of alteration (a regular cobblestone epidermis, a ringed junctional architecture and no atypical cells in the dermis), suggestive of healthy skin. However, the authors recommend that the blue pigmentation, suggestive of a deep dermotropic lesion, where alteration is not visible due to the limited RCM penetration depth, requires biopsy.

Due to the nodular and ulcerated appearance of many dermotropic CMMM lesions, RCM images can be difficult to achieve, and are therefore less likely to be assessed with RCM. Alternatively, epidermotropic CMMMs are less frequently nodular and RCM image acquisition is simplified, and in these cases differential diagnosis from benign lesions (such as nevi) is more frequently required. As the inclusion criteria specified RCM image acquisition, the proportion of epidermotropic and dermotropic lesions in this study does not represent incidence rates; estimates in literature of epidermotropic CMMMs with histological diagnosis represent around 5% of all CMMMs.[14,15]

The current study is mainly limited by the absence of a control group. Prospective comparative studies will be necessary to assess the current findings in terms of differential diagnosis from other skin lesions. Further, the limitations inherent in the cluster methodology restrict this study's applicability to the clinical setting. As grouping is performed according to parameters, outcomes provide information of a biological nature rather than diagnostic. Additionally, information concerning the stage of the disease, the primary tumour location and other clinical history, reported by Plaza *et al.*[14] as helpful in establishing correct histologic diagnosis were not considered in the current study, and could assist in a more detailed analysis of RCM parameters.

This study suggests that RCM seems able to help diagnose most CMMMs and RCM criteria seem different for dermotropic and epidermotropic CMMMs. CMMMs classified at dermoscopy with nevus-like globular and non-globular patterns are more likely to be epidermotropic showing characteristics of epidermal and dermal involvement, and other dermoscopy pattern classifications were more likely to be dermotropic. However, some RCM featureless, non-specific lesions (atypical features in the deep dermis, classified dermoscopically blue-nevus like) cannot be diagnosed with RCM, due to the technology's limited penetration depth, and skin biopsy is always recommended.

References

1 Mohr P, Eggermont AM, Hauschild A, Buzaid A. Staging of cutaneous melanoma. *Ann Oncol* 2009; **20**(Suppl 6): 14–21.
2 Savoia P, Fava P, Nardò T, Osella-Abate S, Quaglino P, Bernengo MG. Skin metastases of malignant melanoma: a clinical and prognostic survey. *Melanoma Res* 2009; **19**: 321–326.
3 Rubegni P, Lamberti A, Mandato F *et al.* Dermoscopic patterns of cutaneous melanoma metastases. *Int J Dermatol* 2014; **53**: 404–412.
4 Bono R, Giampetruzzi AR, Concolino F *et al.* Dermoscopic patterns of cutaneous melanoma metastases. *Melanoma Res* 2004; **14**: 367–373.
5 Pizzichetta MA, Canzonieri V, Gatti A *et al.* Dermoscopic features of metastases from cutaneous melanoma mimicking benign nevi and primary melanoma. *J Clin Oncol* 2002; **20**: 1412–1415.
6 Brauer JA, Wriston CC, Troxel AB *et al.* Characteristics associated with early and late melanoma metastases. *Cancer* 2010; **116**: 415–423.
7 Yu LL, Heenan PJ. The morphological features of locally recurrent melanoma and cutaneous metastases of melanoma. *Hum Pathol* 1990; **30**: 551–555.
8 Schulz H. Epiluminescence microscopy features of cutaneous malignant melanoma metastases. *Melanoma Res* 2000; **10**: 273–280.
9 Jaimes N, Halpern JA, Puig S *et al.* Dermoscopy: an aid to detection of amelanotic cutaneous melanoma metastases. *Dermatol Surg* 2012; **38**: 1437–1444.
10 Minagawa A, Koga H, Sakaizawa K *et al.* Dermoscopic and histo- pathological findings of polymorphous vessels in amelanoticcuta- neous metastasis of pigmented cutaneous melanoma. *Br J Dermatol* 2009; **160**: 1134–1136.
11 Heenan PJ, Clay CD. Epidermotropic metastatic melanoma simulating multiple primary melanomas. *Am J Dermatopathol* 1991; **13**: 396–402.
12 Abernethy JL, Soyer HP, Kerl H *et al.* Epidermotropic metastatic malignant melanoma simulating melanoma in situ. A report of 10 examples from two patients. *Am J Surg Pathol* 1994; **18**: 1140–1149.
13 Ruhoy SM, Prieto VG, Eliason SL *et al.* Malignant melanoma with paradoxical maturation. *Am J Surg Pathol* 2000; **24**: 1600–1614.
14 Plaza JA, Torres-Cabala C, Evans H, Diwan HA, Suster S, Prieto VG. Cutaneous metastases of malignant melanoma: a clinicopathologic study of 192 cases with emphasis on the morphologic spectrum. *Am J Dermatopathol* 2010; **32**: 129–136.
15 Lestre S, João A, Ponte P *et al.* Intraepidermal epidermotropic metastatic melanoma: a clinical and histopathological mimicker of melanoma in situ occurring in multiplicity. *J Cutan Pathol* 2011; **38**: 514–520.
16 Watanabe T, Higaki H, Yamada N, Yoshida Y, Yamamoto O. Dermoscopic and histopathological findings of epidermotropic metastatic malignant melanoma. *Eur J Dermatol* 2011; **21**: 811–813.
17 Skala SL, Arps DP, Zhao L *et al.* Comprehensive histopathological comparison of epidermotropic/dermal metastatic melanoma and primary nodular melanoma. *Histopathology* 2018; **72**: 472–480.
18 Costa J, Ortiz-Ibañez K, Salerni G *et al.* Dermoscopic patterns of melanoma metastases: interobserver consistency and accuracy for metastasis recognition. *Br J Dermatol* 2013; **169**: 91–99.
19 Longo C, Zalaudek I, Argenziano G, Pellacani G. New directions in dermatopathology: in vivo confocal microscopy in clinical practice. *Dermatol Clin* 2012; **30**: 799–814.
20 Longo C, Farnetani F, Ciardo S *et al.* Is confocal microscopy a valuable tool in diagnosing nodular lesions? A study of 140 cases. *Br J Dermatol* 2013; **169**: 58–67.
21 Segura S, Pellacani G, Puig S *et al.* In vivo microscopic features of nodular melanomas: dermoscopy, confocal microscopy, and histopathologic correlates. *Arch Dermatol* 2008; **144**: 1311–1320.
22 Pellacani G, Cesinaro A, Seidenari S. In vivo assessment of melanocytic nests in naevi and melanomas by reflectance confocal microscopy. *Mod Pathol* 2005; **18**: 469–474.

23 Pellacani G, Cesinaro A, Seidenari S. Reflectance-mode confocal microscopy for the in vivo characterization of pagetoid melanocytosis in melanomas and naevi. *J Invest Dermatol* 2005; **125**: 532–537.
24 Gill M, Longo C, Farnetani F, Cesinaro AM, González S, Pellacani G. Non-invasive in vivo dermatopathology: identification of reflectance confocal microscopic correlates to specific histological features seen in melanocytic neoplasms. *J Eur Acad Dermatol Venereol* 2014; **28**: 1069–1078.
25 Pellacani G, Scope A, Farnetani F *et al.* Towards an in vivo morphologic classification of melanocytic nevi. *J Eur Acad Dermatol Venereol* 2014; **28**: 864–872.
26 De Pace B, Farnetani F, Losi A *et al.* Reinterpreting dermoscopic pigment network with reflectance confocal microscopy for identification of melanoma-specific features. *J Eur Acad Dermatol Venereol* 2017; **32**: 947–955.
27 Borsari S, Pampena R, Lallas A *et al.* Clinical Indications for use of reflectance confocal microscopy for skin cancer diagnosis. *JAMA Dermatol* 2016; **152**: 1093–1098.
28 Pellacani G, Pepe P, Casari A, Longo C. Reflectance confocal microscopy as a second-level examination in skin oncology improves diagnostic accuracy and saves unnecessary excisions: a longitudinal prospective study. *Br J Dermatol* 2014; **171**: 1044–1051.
29 Guitera P, Pellacani G, Longo C, Seidenari S, Avramidis M, Menzies SW. In vivo reflectance confocal microscopy enhances secondary evaluation of melanocytic lesions. *J Invest Dermatol* 2009; **129**: 131–138.
30 Farnetani F, Scope A, Coco V *et al.* Paradigmatic cases of pigmented lesions: How to not miss melanoma. *J Dermatol* 2016; **43**: 1433–1437.
31 Calinski RB, Harabasz J. A dendrite method for cluster analysis. *Comm Stat* 1974; **3**: 1–27.
32 Liao M, Li Y, Kianifard F, Obi E, Arcona S. Cluster analysis and its application to healthcare claims data: a study of end-stage renal disease patients who initiated hemodialysis. *BMC Nephtology* 2016; **17**: 25.
33 Perrot JL, Labeille B, Habougit C *et al.* The role of reflectance confocal microscopy in the diagnosis of cutaneous melanoma metastasis. *Ann Dermatol Venereol* 2016; **143**: 863–865.
34 Pellacani G, De Pace B, Reggiani C *et al.* Distinct melanoma types based on reflectance confocal microscopy. *Exp Dermatol* 2014; **23**: 414–418.
35 Pellacani G, Cesinaro AM, Seidenari S. In vivo confocal reflectance microscopy for the characterization of melanocytic nests and correlation with dermoscopy and histology. *Br J Dermatol* 2005; **152**: 384–386.
36 Farnetani F, Scope A, Braun RP *et al.* Skin cancer diagnosis with reflectance confocal microscopy: reproducibility of feature recognition and accuracy of diagnosis. *JAMA Dermatol* 2015; **151**: 1075–1080.

Supporting information

Additional supporting information may be found online in the Supporting Information section at the end of the article.

Figure S1. The dendrogram illustrates how clusters were made by the agglomerative technique; each subject is considered a cluster by itself, and all subjects are then continuously merged together based on similarity between clusters.

Table S1. RCM criteria for melanocytic lesions.

Table S2. Conditions to determine the optimal number of clusters.